

See discussions, stats, and author profiles for this publication at: <https://www.researchgate.net/publication/51128990>

Electron Spin Relaxation and Heterogeneity of the 1:1 α,γ -Bisdiphenylene- β -phenylallyl (BDPA)/Benzene Complex

ARTICLE in THE JOURNAL OF PHYSICAL CHEMISTRY B · JUNE 2011

Impact Factor: 3.3 · DOI: 10.1021/jp201978w · Source: PubMed

CITATIONS

11

READS

32

8 AUTHORS, INCLUDING:



Deborah G Mitchell

University of Denver

20 PUBLICATIONS 186 CITATIONS

SEE PROFILE



Richard W Quine

University of Denver

76 PUBLICATIONS 1,310 CITATIONS

SEE PROFILE



Virginia M Meyer

The National Institute of Diabetes and Digestive and Kidney Diseases

14 PUBLICATIONS 108 CITATIONS

SEE PROFILE



Gareth R Eaton

University of Denver

364 PUBLICATIONS 6,620 CITATIONS

SEE PROFILE

Electron Spin Relaxation and Heterogeneity of the 1:1 α,γ -Bisdiphenylene- β -phenylallyl (BDPA)/Benzene Complex

Deborah G. Mitchell,[†] Richard W. Quine,[‡] Mark Tseitlin,[†] Ralph T. Weber,[§] Virginia Meyer,[†] Azure Avery,[⊥] Sandra S. Eaton,^{*,†} and Gareth R. Eaton[†]

[†]Department of Chemistry and Biochemistry, University of Denver, Denver, Colorado 80208, United States

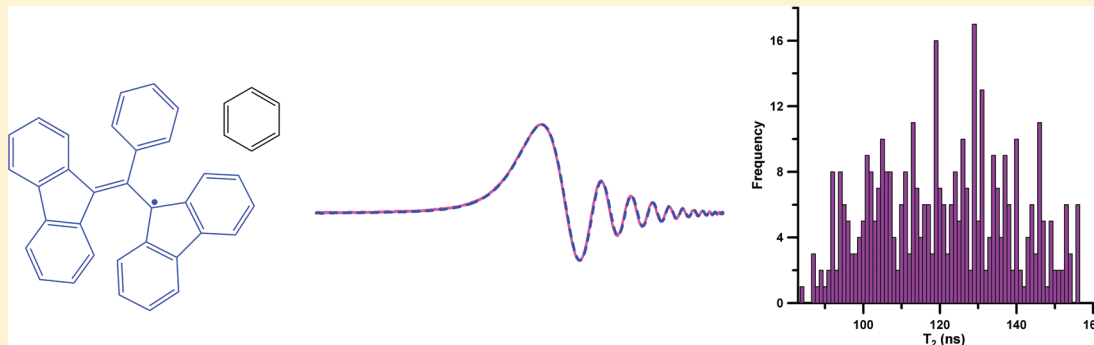
[‡]School of Engineering and Computer Science, University of Denver, Denver, Colorado 80208, United States

[§]Bruker BioSpin, Billerica, Massachusetts 01821, United States

[⊥]Department of Physics and Astronomy, University of Denver, Denver, Colorado 80208, United States

S Supporting Information

ABSTRACT:



The electron spin–spin relaxation time (T_2) for the 1:1 crystalline complex of α,γ -bisdiphenylene- β -phenylallyl (BDPA) with benzene was determined by continuous wave (CW) and rapid scan electron paramagnetic resonance (EPR). T_2 for individual BDPA particles found by simulation of rapid scan spectra or by simulation of the Lorentzian line shapes of CW spectra were in good agreement. The T_2 for small BDPA particles in air ranged from 80 to 160 ns, which corresponds to peak-to-peak Lorentzian linewidths of 0.82–0.41 G. The removal of oxygen from the samples had a greater impact on the line width for particles that had shorter T_2 in air. Heterogeneity in the g -value was not observed at X-band. Scanning electron microscope (SEM) images showed that the BDPA particles had varying morphology.

1. INTRODUCTION

The stable organic radical BDPA (α,γ -bisdiphenylene- β -phenylallyl) is widely used in dynamic nuclear polarization NMR studies.^{1,2} Because of its intense electron paramagnetic resonance (EPR) signal, magnetically concentrated solid BDPA has been used in the development of novel methods to study unpaired electrons.^{3–6} In this paper rapid scan and CW (continuous wave) EPR at X-band were used to determine electron spin–spin relaxation times at room temperature for the commercially available crystalline 1:1 BDPA/benzene complex,⁷ in which the benzene stabilizes the radical. Experiments were performed to determine the impact of oxygen and benzene on relaxation times.

When the line shape of an EPR signal is a relaxation-determined Lorentzian, the spin–spin relaxation time T_2 can be determined directly from the peak-to-peak continuous wave (CW) line width. However, it can be difficult to distinguish a narrow distribution of Lorentzian lineshapes from a single Lorentzian. For very narrow

lines there also is a problem that 100 kHz magnetic field modulation can broaden the CW line shape even when the modulation amplitude is much less than the line width. Rapid scan EPR spectra are strongly dependent on T_2 and therefore provide an alternate method to determine T_2 . In rapid scan EPR the magnetic field is swept through resonance in a time that is short relative to relaxation times, which causes oscillations on the trailing edge of the signal. The oscillations damp out with a time constant that depends on T_2 and on inhomogeneous broadening,^{8–10} which permits the determination of T_2 by simulation of the rapid scan spectra.⁸ Rapid scan measurements of T_2 can be performed without the need for the high microwave powers used in pulsed EPR and without the magnetic field modulation that can broaden conventional CW spectra. To achieve rapid scan conditions for the BDPA samples, rates greater

Received: March 1, 2011

Revised: May 13, 2011

Published: May 16, 2011

than about 10 MG/s are required. These rapid sinusoidal scan rates were achieved by using the electron–nuclear double resonance (ENDOR) coils in a Bruker ER 4118X-MD4 pulse ENDOR resonator, rotated by 90° to align the radio frequency (rf) field with the static magnetic field.¹¹ Rapid scan EPR spectra can be deconvolved to recover the slow scan (CW) spectrum.^{8,12}

2. METHODS

2.1. Samples. The 1:1 BDPA/benzene complex was purchased from Sigma Aldrich (batch #00226KM). Small particles of BDPA were selected and placed in 0.8 mm inner diameter (i.d.) Pyrex capillaries, which were supported in 4 mm outer diameter (o.d.) quartz EPR tubes. Most experiments were performed with air-saturated samples. For rapid scan experiments, ~0.1 mL of a 3:1 (by weight) ethanol–water mixture was placed in the annulus surrounding the capillary containing the BDPA sample, to lower resonator *Q* to about 200. If resonator *Q* is not sufficiently low, the limited resonator bandwidth may dominate the damping of the rapid scan oscillations.

Oxygen and benzene were removed from selected BDPA samples to determine the impact on the CW line width and on electron spin–spin relaxation times. To remove oxygen, samples were evacuated for about 5 h, without heating. To remove benzene,¹³ samples were evacuated while heating at 90 °C for about 7 h. To characterize BDPA with reduced benzene content in the presence of air, air was reintroduced after the samples had cooled.

UV–vis experiments were performed to determine if variations in *T*₂ were due to impurities in the samples. *T*₂ was determined from CW lineshapes for 386 individual small BDPA particles. The distribution of *T*₂ is shown in Figure S1 of the Supporting Information. The particles were sorted, based on *T*₂, into separate containers. A total of 1.0 mg of BDPA from containers with *T*₂ in four ranges (102–107 ns, 112–117 ns, 122–125 ns, 137–142 ns) was dissolved in chloroform to make four solutions with 30 μM concentrations. UV–vis spectra were collected on a Varian Cary 100 Bio UV–vis spectrometer with a wavelength range of 200–900 nm.

To determine if particles with different *T*₂ had different physical characteristics, scanning electron microscope (SEM) images of selected BDPA particles were collected. Particles were placed in silver paint, and SEM images were collected on a JEOL JSM-IC848a microscope.

2.2. EPR Spectroscopy. Rapid scan signals were recorded on a Bruker E500T transient X-band spectrometer. The microwave bridge has a 200 MHz bandwidth video amplifier. Signal acquisition was via a SpecJet II digitizer. A critically coupled Bruker ER4118X-MD4 pulse ENDOR resonator was rotated such that the field resulting from the ENDOR coils was parallel to the *B*₀ magnetic field. Resonator *Q* was measured using pulse ring down with a locally designed addition to the bridge¹⁴ and with an HP 8719D network analyzer. To avoid excess heating of the ENDOR coils, the sine wave for the magnetic field scans was generated with a Tektronix AWG2021 arbitrary waveform generator, operating in burst mode. The duty cycle was about 1%. The center field was selected to be close to resonance. The scan rate at the center of a sinusoidal scan, which is used to describe spectra, is given by eq 1,

$$\text{rate} = \pi w f \quad (1)$$

where *w* is the width of the sinusoidal scan (in gauss) and *f* is the scan frequency. For the BDPA experiments scan frequencies ranged from 300 kHz to 1.5 MHz and scan widths varied from

17 to 60 G. This corresponds to rates at the center of the scan of 16–280 MG/s. The ENDOR coils can be used to generate sweep widths up to 70 G peak-to-peak at scan frequencies up to 5 MHz, which corresponds to scan rates in excess of 1 GG/s. However, these rates are higher than are needed to characterize *T*₂ of BDPA and would have required significant decrease in resonator *Q* to record spectra with sufficient signal bandwidth.

The slow scan spectra were recovered from the rapid scan signals using Fourier deconvolution.¹² The first derivatives of the absorption signals recovered from the rapid scans were calculated using a function analogous to the pseudomodulation method described by Hyde et al.¹⁵ and included a Butterworth filter to approximate the impact of the spectrometer time constant.

To define the distribution of *T*₂ shown in Figure S1 of the Supporting Information, CW spectra of small BDPA particles were collected on a Bruker EMX-plus X-band spectrometer at room temperature with a sweep width of 10 G, modulation frequency of 100 kHz, and modulation amplitude of 0.08 G. The 100 kHz modulation frequency was used for convenience, although it caused some broadening of the narrowest lines. For the more precise comparisons of lineshapes with deconvolved rapid-scan spectra, CW spectra were obtained with a modulation frequency of 30 kHz.

2.3. Simulations. CW spectra were simulated with a Lorentzian line shape using the shareware package Easyspin.¹⁶ *T*₂ was calculated using eq 2, which is valid only for unsaturated spectra with a Lorentzian line shape that is relaxation determined.

$$\Delta B_{\text{pp}} = \frac{2}{\sqrt{3}\gamma T_2} = \frac{6.56 \times 10^{-8} \text{ G}}{T_2} \quad (2)$$

where ΔB_{pp} is the peak-to-peak line width for the EPR first derivative signal, γ is the electron gyromagnetic ratio, and *T*₂ is the spin–spin relaxation time. The simulations of the CW spectra are fairly sensitive to *T*₂, with an uncertainty of about 2–3%. The uncertainty is based on the range of linewidths that appear to give similar agreement with the experimental data.

Simulations of the rapid scan signals were performed by numerical integration of the Bloch equations⁸ using a program written in MATLAB. The input parameters are magnetic field scan width, scan frequency, resonator *Q*, offset of the center of the scan from the resonant magnetic field, and *T*₂ relaxation time. For these simulations, all parameters were known except *T*₂, which was adjusted to fit the spectra. The uncertainty in *T*₂, about ±5%, was calculated from the confidence level of replicate measurements, converted to a percent. Factors that contribute to the uncertainty are variations in background and uncertainty in the value of resonator *Q*. Uncertainties are greater for samples with weaker signals. *T*₂ obtained by simulation of the rapid scan spectra was compared to *T*₂ calculated from the CW linewidths. Agreement between the results obtained by the two methods indicates that systematic sources of error have been minimized.

3. RESULTS

3.1. EPR Spectra of BDPA. Although commercial BDPA is a crystalline solid, the particles do not appear to be single crystals, and there is a wide range of morphology. Therefore in the following discussion the designation “particle” is used instead of “crystal”. Rapid scan experiments using multiple particles resulted in spectra that could not be simulated with a single *T*₂. Therefore attention was focused on individual particles and characterization of the differences among particles.

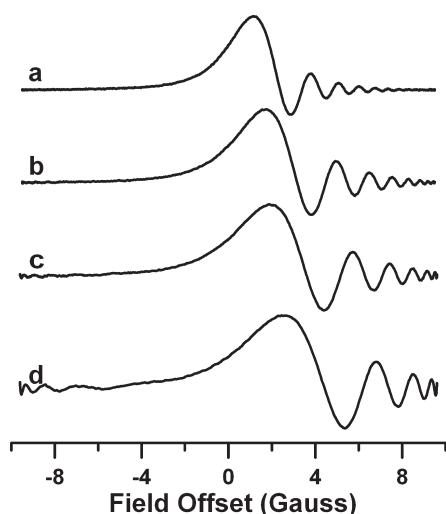


Figure 1. Rapid scan spectra of a BDPA particle with $T_2 = 88 \pm 3$ ns, obtained with constant 19 G scan width, and different scan frequencies. 10240 averages were collected with resonator $Q \sim 200$ and 0.2 mW power. (a) 300 kHz scan frequency (18 MG/s), recorded in ~ 30 s. (b) 500 kHz scan frequency (30. MG/s), recorded in ~ 20 s. (c) 700 kHz scan frequency (42 MG/s), recorded in ~ 15 s. (d) 1 MHz scan frequency (60 MG/s), recorded in ~ 10 s.

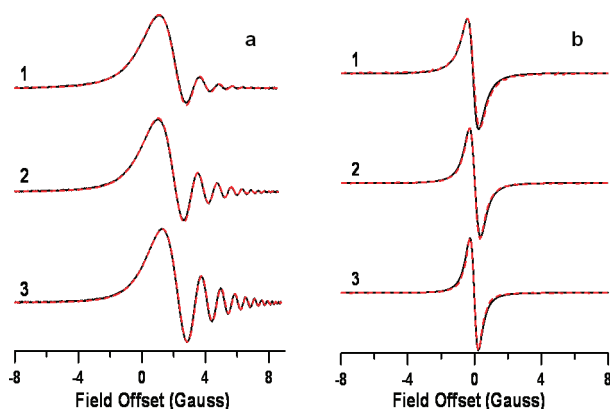


Figure 2. (a) Rapid scan EPR (black line) of BDPA particles 1–3 (with $T_2 = 85$, 110, and 141 ns, respectively) and simulations (red dashed line). Spectra were collected with resonator $Q \sim 200$, 300 kHz scan frequency, 17.2 G scan width, scan rate 16.25 MG/s, 0.2 mW power, and 10240 (samples 1 and 3) or 20480 scans (sample 2). (b) Comparison of CW spectra (black line) with first derivative spectra obtained by pseudomodulation from the deconvolved rapid scan spectra (red line). CW spectra were collected with 30 kHz modulation frequency, 0.08 G modulation amplitude, and 0.02 mW power. For sample 1, four averages were recorded in about 5.5 min. For samples 2 and 3, a single scan was recorded in 86 s.

Sinusoidal rapid scans of a BDPA particle at scan rates in the center of the scan of 18–60 MG/s are shown in Figure 1. The absorption signals are recorded by direct detection. As the scan rate increases, the signal broadens, the amplitude of the oscillations increases, and the number of oscillations increases.¹⁷ The spacing between the peaks in the oscillation decreases as the magnetic field is scanned above or below resonance. The time constant for the damping is T_2 , which was determined by simulation.

Rapid scan spectra for BDPA particles 1–3, which have different T_2 , recorded at a rate in the center of the scan of 16.25 MG/s are shown in Figure 2a. The shorter the T_2 , the more

Table 1. T_2 (ns) for Three BDPA Particles for Which Spectra Are Shown in Figure 2

particle	T_2 from rapid scan EPR ^a	T_2 from CW EPR ^b
1	85	92
2	110	103
3	141	130

^a The average uncertainty, calculated for replicate rapid scan measurements, was $\pm 5\%$. ^b The average uncertainty, calculated for replicate CW measurements, was $\pm 2\%$.

Table 2. Effect of Oxygen and Benzene on the Linewidths (G) for Four Samples

particle	4	5	6	7
original in air	0.68	0.53	0.49	0.42
evacuated ^a	0.35	0.36	0.40	0.42
no benzene or O ₂	0.38	0.28–1.5 ^b	0.36–1.4 ^b	0.5–1.2 ^b
no benzene, w/air	1.8	0.7–1.9 ^b	1.6	1.5

^a Evacuated for 4 h at ambient temperature to remove O₂. ^b These line shapes could not be fit with single Lorentzians but appeared to be superpositions of multiple Lorentzians with widths in the tabulated range.

quickly the oscillation decays. The effects of the sinusoidal rapid scan on the EPR signals in Figure 2a can be deconvolved to recover the slow scan lineshapes, as shown in Figure 2b. The slow scan lineshapes obtained by deconvolution and conversion to the first-derivative display are in excellent agreement with traditionally recorded CW spectra obtained with 30 kHz modulation frequency. The use of 100 kHz modulation frequency for the CW spectra of BDPA causes small, but significant, broadening, which became evident when the values of T_2 obtained by rapid scan and CW lineshapes were compared. T_2 determined from rapid scan and CW spectra for the three samples for which data are shown in Figure 2 are compared in Table 1.

3.2. Effect of Oxygen and Benzene on Relaxation Times for BDPA Particles. CW spectra were recorded for four BDPA samples that had been evacuated to remove oxygen and subsequently heated in vacuum to remove benzene. The samples were selected to have different initial linewidths in air. Table 2 shows the changes in the CW linewidths that were observed. Removal of oxygen caused the largest decrease in line width for particle 4, which had the broadest initial line width. For particle 4, heating under vacuum to remove benzene caused little additional change in line width. For the other particles heating under vacuum resulted in distributions of linewidths and formation of components with substantially broadened lines. For all of the heated particles, exposure to air caused substantial broadening of the lines. The changes due to heating in vacuum were not reversible.

3.3. UV–vis of BDPA in CHCl₃ and SEM Images. UV–vis spectra were recorded for BDPA particles with different ranges of T_2 (102–107 ns, 112–117 ns, 122–127 ns, 137–142 ns) dissolved in CHCl₃ (Figure S2 of the Supporting Information). Each sample had $\lambda_{\text{max}} = 488$ nm and a weaker absorbance at $\lambda = 874$ nm, which is in good agreement with the literature,¹ and there was no evidence of peaks characteristic of the diamagnetic carbanion precursor.

The SEM images of two different BDPA particles ($T_2 \sim 96$ ns and $T_2 \sim 152$ ns) are shown in the Supporting Information, Figures S3–S8.

4. DISCUSSION

4.1. Determining T_2 of BDPA through Simulations and Comparison with CW. The exchange-narrowed line shape for solid 1:1 BDPA/benzene in the presence or absence of air (O_2) is Lorentzian, so T_2 can be calculated from the CW line width. Simulations with a Lorentzian line shape were in reasonable agreement with experimental spectra of samples consisting of multiple particles. However, rapid scan experiments using multiple particles resulted in spectra that could not be simulated with a single T_2 . This result indicated that the BDPA sample could not be represented by a single spin packet and was actually a distribution of spin packets. From these simulations, rapid scan EPR provided information about BDPA that was not evident in the CW experiments. Although it might be expected that electron spin echo experiments would be helpful in determining T_2 , the homogeneous broadening of the lines precluded echo formation. Common techniques of creating a gradient across a sample to facilitate echo formation were unsuccessful because of the very small sizes of the particles.

Figure 2a illustrates that rapid scan EPR spectra are sensitive to the T_2 of a sample. The T_2 required to simulate the rapid scan spectra for individual particles matched well with T_2 determined from the line width of the CW spectrum obtained with 30 kHz modulation frequency (see Table 1). The rapid scan spectra also were deconvolved to obtain the slow scan spectrum. The first derivative of the deconvolved rapid scan spectra for particles 1, 2, and 3 agreed well with the conventionally recorded CW spectra (see Figure 2b).

4.2. Heterogeneity of BDPA. Individual BDPA particles have T_2 relaxation times ranging from 80–160 ns (Figure S1). The distribution in T_2 does not appear to be Gaussian so it is attributed to variations in physical properties. At X-band there does not appear to be a distribution in g values. Rotation of a particle with a goniometer through 180° found line width variation only between 0.49 and 0.44 G. This small orientation dependence indicates that the distribution of linewidths implied by the relaxation times in Figure S1 is not simply due to different orientations of the particles in the magnetic field. Data in Table 2 show that BDPA particles with a variety of T_2 are affected differently by the removal of oxygen as well as removal of both benzene and oxygen. BDPA particles with shorter T_2 are more sensitive to the removal of oxygen. These differences may be due to morphology and/or benzene concentration. For the oximetric probe lithium phthalocyanine (LiPc) there is a correlation between sensitivity to oxygen and crystal morphology.¹⁸ SEM images (see Figures S3–S8 of the Supporting Information) indicate that the BDPA particles have many different crystal morphologies. However, there does not appear to be a correlation between the shape of the particle and the T_2 for the particle.

It is important to note that evacuation of BDPA with or without heating to remove benzene was not a reversible process for these particles. After removal of benzene and exposure to air, the lines for all samples are broader and linewidths are more heterogeneous than before evacuation. The irreversibility of evacuation indicates that structural changes are occurring.

5. CONCLUSIONS

The commercial BDPA complex with benzene (1:1) has different T_2 for various particles, which was first evident from the rapid scan spectra. The rapid-scan spectroscopy gave us

insight into the spin–spin relaxation of BDPA that was not obvious from CW techniques alone. Heterogeneity in the g -value of BDPA particles was not evident at X-band. We hypothesize that the BDPA particles have differing T_2 due to differences in crystal morphology and/or the ratio of benzene/BDPA in the crystal, which impact the effectiveness of spin exchange. BDPA is a stable organic radical that has an intense signal and is therefore appealing as a standard in EPR experiments and for use in DNP. However, rapid scan spectra and CW experiments have demonstrated that the commercial 1:1 BDPA/benzene complex is a heterogeneous sample. If BDPA is chosen as a standard during the development of a new method, the heterogeneity of the material should be taken into account.

■ ASSOCIATED CONTENT

S Supporting Information. Figure S1 describing the distribution in T_2 for BDPA. UV–vis spectrum of BDPA dissolved in chloroform (Figure S2). SEM images (Figures S3–S8) of two different BDPA particles, which illustrate morphology of BDPA particles. This material is available free of charge via the Internet at <http://pubs.acs.org>.

■ AUTHOR INFORMATION

Corresponding Author

*University of Denver, Department of Chemistry and Biochemistry, Denver, CO 80208. Phone: 303-871-3102. Fax: 303-871-2254.

■ ACKNOWLEDGMENT

This work was supported in part by NSF IDBR 0753018 and by an NSF Graduate Fellowship to DGM.

■ REFERENCES

- (1) Dane, E. L.; Swager, T. M. *J. Org. Chem.* **2010**, *75*, 3533–3536.
- (2) Giraudeau, P.; Shrot, Y.; Frydman, L. *J. Am. Chem. Soc.* **2009**, *131*, 13902–13903.
- (3) Bennati, M.; Farrar, C. T.; Bryant, J. A.; Inati, S. J.; Weis, V.; Gerfen, G. J.; Riggs-Gelasco, P.; Stubbe, J.; Griffin, R. G. *J. Magn. Reson.* **1999**, *138*, 232–243.
- (4) Goldfarb, D.; Lipkin, Y.; Potapov, A.; Gorodetsky, Y.; Epel, B.; Raitsimring, A. M.; Radoul, M.; Kaminker, I. *J. Magn. Reson.* **2008**, *194*, 8–15.
- (5) Durkan, C.; Welland, M. E. *Appl. Phys. Lett.* **2002**, *80*, 458–460.
- (6) Koksharov, Y. A.; Bykov, I. V.; Malakho, A. P.; Polyakov, S. N.; Khomutov, G. B.; Bohr, J. *Mater. Sci. Eng. C* **2002**, *22*, 201–207.
- (7) Williams, D. E. *J. Am. Chem. Soc.* **1967**, *89*, 4280–4287.
- (8) Joshi, J. P.; Ballard, J. R.; Rinard, G. A.; Quine, R. W.; Eaton, S. S.; Eaton, G. R. *J. Magn. Reson.* **2005**, *175*, 44–51.
- (9) Dadok, J.; Sprecher, R. F. *J. Magn. Reson.* **1974**, *13*, 243–248.
- (10) Gupta, R. K.; Ferretti, J. A.; Becker, E. D. *J. Magn. Reson.* **1974**, *16*, 505–507.
- (11) Kälén, M.; Gromov, I.; Schweiger, A. *J. Magn. Reson.* **2003**, *160*, 166–182.
- (12) Tseitlin, M.; Rinard, G. A.; Quine, R. W.; Eaton, S. S.; Eaton, G. R. *J. Magn. Reson.* **2011**, *208*, 279–283.
- (13) Yamauchi, J.; Adachi, K.; Deguchi, Y. *Chem. Lett.* **1972**, *1*, 733–735.
- (14) Quine, R. W.; Mitchell, D.; Eaton, G. R. *Magn. Reson. Eng.* **2011**, *39B*, 43–46.
- (15) Hyde, J. S.; Jesmanowicz, A.; Ratke, J. J.; Antholine, W. E. *J. Magn. Reson.* **1992**, *96*, 1–13.

- (16) Stoll, S.; Schweiger, A. *J. Magn. Reson.* **2006**, *178*, 42–55.
- (17) Stoner, J. W.; Szymanski, D.; Eaton, S. S.; Quine, R. W.; Rinard, G. A.; Eaton, G. R. *J. Magn. Reson.* **2004**, *170*, 127–135.
- (18) Ilangoan, G.; Zweier, J. L.; Kuppusamy, P. *J. Phys. Chem. B* **2000**, *104*, 9404–9410.